# The evidence of porcine hemagglutinating encephalomyelitis virus induced nonsuppurative encephalitis as the cause of death in piglets

Zi Li[1][*], Wenqi He[1][*], Yungang Lan[1], Kui Zhao[1], Xiaoling Lv[1], Huijun Lu[2], Ning Ding[1], Jing Zhang[1], Junchao Shi[1], Changjian Shan[1], Feng Gao[1][#]

[1] Key Laboratory of Zoonosis, Ministry of Education, College of Veterinary Medicine, Jilin University. Changchun, Jilin, China.

[2] Key Laboratory of Zoonosis, Ministry of Education, Institute of Zoonosis, Jilin University, Changchun, Jilin, China.

Corresponding Author:

Feng Gao[1]

5333 Xi'an Road, Changchun, Jilin, 130062, China

Street Address, City, State/Province, Zip code, Country

Email address: gaofeng@jlu.edu.cn

*They contributed equally to this work.

20   **Abstract**

21       An acute outbreak of porcine hemagglutinating encephalomyelitis virus (PHEV) infection in

22   piglets, characterized with neurological symptoms, vomiting, diarrhea, and wasting, occurred in

23   China. Coronavirus-like particles were observed in the homogenized tissue suspensions of the

24   brain of dead piglets by electron microscopy, and a wild PHEV strain was isolated, characterized,

25   and designated as PHEV-CC14. Histopathologic examinations of the dead piglets showed

26   characteristics of non-suppurative encephalitis, and some neurons in the cerebral cortex were

27   degenerated and necrotic, and neuronophagia. Similarly, mice inoculated with PHEV-CC14 were

28   found to have central nervous system (CNS) dysfunction, with symptoms of depression, arched

29   waists, standing and vellicating front claws. Furthmore, PHEV-positive labeling of neurons in

30   cortices of dead piglets and infected mice supported the viral infections of the nervous system.

31   Then, the major structural genes of PHEV-CC14 were sequenced and phylogenetically analyzed,

32   and the strain shared 95%-99.2% nt identity with the other PHEV strains available in GenBank.

33   Phylogenetic analysis clearly proved that the wild strain clustered into a subclass with a HEV-

34   JT06 strain. These findings suggested that the virus had a strong tropism for CNS, in this way,

35   inducing nonsuppurative encephalitis as the cause of death in piglets. Simultaneously, the

36   predicted risk of widespread transmission showed a certain variation among the PHEV strains

37   currently circulating around the world. Above all, the information presented in this study can not

38   only provide good reference for the experimental diagnosis of PHEV infection for pig breeding,

39   but also promote its new effective vaccine development.

40   **Introduction**

41    Porcine hemagglutinating encephalomyelitis virus (PHEV) belongs to the order *Nidovirales*,

42    family *Coronaviridae*, and genus *Coronavirus*, and causes encephalomyelitis or vomiting and

43    wasting disease in suckling piglets (Andries & Pensaert 1981; Mengeling et al. 1972). Previous

44    studies have demonstrated that the virus has a strong tropism for the upper respiratory tract and is

45    propagated through the neural route (Andries & Pensaert 1980). The disease caused by PHEV

46    was first reported in Canada in 1958 (Roe & Alexander 1958), and the pathogen was first

47    isolated from the brains of suckling piglets with encephalomyelitis in 1962 (Greig et al. 1962).

48    Since then, the infection has been reported in the United States, Japan, Argentina, Belgium,

49    South Korea, China and other pig-raising countries (Gao et al. 2011; Hirano & Ono 1998;

50    Pensaert & Callebaut 1974; Quiroga et al. 2008; Rho et al. 2011; Sasseville et al. 2001). Today,

51    many serological surveys have revealed that PHEV is widespread, and there are frequent

52    subclinical infections (Li et al. 2013).

53    In China, PHEV infection first occurred in Beijing in 1985, and the outbreaks caused

54    enormous economic losses for the pig industry (Chen et al. 2012; Dong et al. 2014; Gao et al.

55    2011). Here we report that there is a suspected outbreak of PHEV infection on a farm in

56    Changchun of Jilin Province, in 2014, resulting in serious economic losses. Many infected

57    piglets characterized with vomiting and nerve symptoms, and some cases were accompanied by

58    screaming or diarrhea; all of the piglets with clinical symptoms died finally. In this paper, the

59    diagnosis was made on the basis of pathologic features, immunohistochemistry, microbiological

60    detection, and RT-PCR. A PHEV field strain was isolated from the brain tissue of infected

61    piglets, and the major structural proteins of the strain were sequenced to identify genetic

62    relationships with other coronaviruses of the genus *Betacoronavirus*.

## Materials & Methods

### Sample collection and testing

On March 2014, there was an acute outbreak of suspected porcine hemagglutinating encephalomyelitis in suckling pigs on a farm with a total of 502 sows in Changchun, Jilin province, China. At the time of the outbreak, these pigs had not been immunized with any PHEV vaccines; the total proportion of deaths in piglets that had not been weaned was 46.7% (140 dead piglets). The collected samples were tested for PHEV using real-time reverse transcription-polymerase chain reaction (RT-PCR) targeting the HE gene, as well as for other viruses that cause similar clinical symptoms among swine, including porcine epidemic diarrhea virus (PEDV), porcine transmissible gastroenteritis virus (TGEV), porcine deltacoronavirus (PDCoV), and pseudorabies virus (PRV). All experiments on piglets research were performed in accordance with Animal Welfare Ethical Committee of Jilin University guidelines and regulations (permission number 2012-CVM-12). The involved RT-PCR primers were designed based on the most conserved segment of their genomes (Table 1), and subsequently validated by BLAST (http://www.ncbi.nlm.nih.gov/BLAST) with sequences from GenBank. The original samples were diluted 10-fold with phosphate-buffered saline (PBS) and were centrifuged at 3,000×g at 4℃ for 10 min. The supernatant was filtered through a 0.22-μm syringe filter, and was used as inoculums for BALB/c mice or for virus isolation in Neuro-2a cell culture.

### Histopathologic examination

82    Postmortem examinations were performed and samples submitted for histopathologic

83    examination, including tissues from the brain, heart, spleen, liver, kidneys, and lungs. Paraffin-

84    embedded sections of brain that had characteristic microscopic lesions were examined by

85    hematoxylin-eosin staining. Selected paraffin sections for PHEV antigen detection by

86    immunohistochemistry (IHC) tests were treated with normal goat serum for 1 hour and anti-HEV

87    67N monoclonal antibody (Chen et al. 2012) (diluted 1:100) overnight; then, the staining

88    procedure was performed according to the kit instructions.

89    **Inoculation of BALB/c mice with PHEV strains**

90    Thirty 3-week-old male BALB/c mice were randomly and equally divided into 3 groups.

91    The mice in group 1 were inoculated with the original filtered brain tissue by the intranasal route,

92    the mice in group 2 were inoculated with HEV 67N (GenBank: AY048917) in the same manner,

93    and the mice in the third group formed a negative control group. The permission to work with

94    laboratory animals was obtained from the Animal Welfare Ethical Committee of the College of

95    Veterinary Medicine, Jilin University, China (permission number 2012-CVM-12). All of the

96    mice experiments were carried out at Bio-Safety Level 2 (BSL-2) facilities at the Key Laboratory

97    of Zoonosis, Ministry of Education, College of Veterinary Medicine, Jilin University. Clinical

98    signs were monitored, and immunofluorescence assay (IFA) was performed. The PHEV

99    monoclonal antibody (diluted 1:500) was used as the primary antibody, and a 1:200 dilution of

100    affinity purified fluorescein-labeled goat anti-mouse IgG was used as the second antibody. Cell

101    staining was examined using a fluorescence microscope.

102 **Virus isolation and propagation**

103      The Neuro-2a cell line was used to isolate PHEV from the original field and from mouse-

104 passaged PHEV samples. Cultured cells were propagated in Dulbecco's Modified Eagle Medium

105 (DMEM, Gibco, USA) supplemented with 10% heat-inactivated fetal bovine serum (Hyclone,

106 Logan, UT, USA) and 1% antibiotic-antimycotic (Gibco, USA). Briefly, a monolayer of cells

107 was washed twice with 2% DMEM, and then was inoculated with the filtered samples. After

108 adsorption for 1 h at 37℃ in 5% $CO_2$, the cells were washed 3 times, and 2% DMEM was added.

109 The cell cultures were examined daily for cytopathic effect (CPE). When more than 80% CPE

110 was evident in the inoculated cell monolayers, the cells and supernatants were harvested together

111 and used as seed stocks for the next passage. After serial passage, the cell cultures were clarified

112 by centrifugation at 3,000 × g for 30 min at 4℃ and then were further ultracentrifuged at 20,000

113 × g for 2 h at 4℃ using an ultracentrifuge. The pellet was resuspended and submitted for

114 virological investigation using electron microscopy (EM). The virus isolate was designated

115 PHEV-CC14.

116 **Virus titration and purification by plaque assay**

117      The 100% confluent Neuro-2a cells in 6-well plates were used for plaque assays of PHEV-

118 CC14 propagation and purification. Briefly, the wells were inoculated with 10-fold serially

119 diluted virus (0.2 mL/well), followed by adsorption for 1 h at 37℃ in 5% $CO_2$; then, the wells

120 were washed 3 times, and 2 mL of the agarose/MEM mixture (1:1) were added. After the plaques

121 were counted and confirmed, uniform and clear plaques were chosen to inoculate 6-well plates

122    directly. When CPE was observed, the positive clones were harvested, and the viral titers were

123    determined. When the Neuro-2a cells were confluent in 96-well plates, 100 mL of 10-fold

124    dilutions of the purified virus were absorbed for 1 h. Viral CPE was monitored for 5 to 7 days,

125    and virus titers were determined by 50% tissue culture infectious dose ($TCID_{50}$).

126    **PHEV-CC14 structural gene sequencing and phylogenetic analysis**

127         All five of the main structural protein genes, hemagglutinin-esterase (HE), spike (S), small

128    membrane (E), membrane (M) and nucleocapsid (N), of PHEV in the original specimen, in the

129    BALB/c mice infected with passaged PHEV-CC14, and in cell culture were amplified, cloned

130    and sequenced. All of the primers were designed according the sequence of the HEV 67N

131    genome. Viral RNA was extracted from the brain tissue suspensions of symptomatic piglets

132    using a commercial kit (QIAGEN, Germany), and the RNA was quantified using a

133    spectrophotometer (BIO-RAD, USA). The RNA was converted to cDNA by an oligo (dT)-

134    priming strategy, and the genes were amplified using PrimeSTAR MAX DNA Polymerase

135    (Takara, Japan). The purified PCR products were cloned into the pMD18-T vector (TaKaRa,

136    Japan) and were introduced into *E. coli* DH5a by transformation. The recombinant plasmids

137    were extracted and verified by PCR and then were sequenced at Shanghai Sangon Biological

138    Engineering Technology and Services Co., Ltd. (China).

139         The sequence data were assembled and analyzed using DNASTAR and NCBI BLAST

140    (http://blast.ncbi.nlm.nih.gov/Blast.cgi). The percentage similarities of the nucleotides and amino

141    acids were analyzed using DNAMAN and DNASTAR software. The structural gene sequences

142     and other coronavirus strains sequence were subjected to phylogenetic analysis using the

143     neighbor-joining method in MEGA software, version 6.06.

144     **Statistical analysis**

145         Statistical analysis was performed with either Student's t-test or one-way ANOVA with a

146     Bonferroni post hoc test with software provided by GraphPad Prism version 5. Data were

147     presented as means ± S.E.M. P values of <0.05 were considered statistically significant.

## Results

### Pathological examination and pathogen detection

Clinical signs of these suspected infected suckling piglets were consisted of vomiting, diarrhea, wasting, dullness, screaming, anorexia, trembling, and ataxia (Fig.1A). Pathological examination showed that the main changes in the piglets were congestion, edema and hemorrhage in brain tissue (Fig.1B). None significant histopathological changes were found in other substantive organs. A total of 54 homogenized tissue suspensions of the brain, spinal cord, lungs, kidneys, spleen and intestinal contents from 9 suspected piglets were tested for PHEV by RT-PCR. Of these tested samples, eight of nine brain samples from young nursing pigs on the farms were PHEV positive, as well as eight of nine spinal cord samples and four of nine intestinal content samples (Table 2). Of the 20 PHEV-positive samples, all were negative for PEDV, TGEV, PDCoV, and PRV.

### Histopathologic examination of the PHEV-infected piglets

Postmortem examinations were performed on 7 infected piglets for pathologic evaluation. Samples submitted for histopathologic examination included brains from PHEV- infected piglets and antigen-negative piglets. Microscopic examination of brain samples showed characteristics of non-suppurative encephalitis. A large number of glial cells were aggregated to glial nodules in the infected brains (Fig.2A and 2B). Neurons in the cerebral cortex were degenerated and necrotic, and neuronophagia was widespread (Fig.2C and 2D). Selected paraffin sections of brain samples that had characteristic microscopic lesions were examined for PHEV antigen by IHC

168  tests with an anti-PHEV monoclonal antibody. In the brains, antigen-positivity in the cytoplasm

169  of nerve cells was distributed widely in the cortical neurons (Fig.2E). Brain samples from the

170  healthy pig were normal (Fig.2F).

171  **Pathogenicity of HEV 67N and PHEV-CC14 in BALB/c mice**

172  Mice in two infected groups were inoculated with HEV 67N and PHEV-CC14, respectively,

173  and were monitored daily for clinical signs of disease. Mice in the HEV 67N-infected group

174  showed typical neurological damage, with symptoms of depression, arched waists, standing and

175  vellicating front claws at 3 days post-inoculation (dpi). The same symptoms occurred in the

176  PHEV-CC14-infected group (Fig.3A and 3B), but the emergence time was slightly delayed

177  (Fig.3C, P<0.05). All of the infected mice died within a week, and the mice in the control group

178  survived normally. Paraffin-embedded sections of the infected mouse brain samples were

179  positive for PHEV in the cytoplasm of nerve cells by IFA using a mouse anti-PHEV monoclonal

180  antibody. In the brain, antigen-positive neurons were distributed widely in the cerebral cortex

181  and hippocampus (Fig.4). In the cerebellum, viral-specific antigen was detected in the Purkinje

182  cells (Fig.4) but in only a few granular cells.

183  **Isolation and purification of PHEV-CC14 strain**

184  The Neuro-2a cell monolayer was inoculated with original field and mouse-passaged PHEV-

185  positive samples. At 3 dpi, the inoculated cell monolayer showed visible CPE, in the form of

186  gathering pyknosis and rounded cells that rapidly detached from the monolayer on 4 dpi (Fig.5B),

187  the mock-inoculated Neuro-2a cells showing normal cells (Fig.5A). The virus was further

188    serially passed in Neuro-2a cells for a total of 18 passages. Virus growth was confirmed by IFA

189    using the antiserum PHEV, and the antigens were mostly located in the cytoplasm (Fig.5C). To

190    confirm PHEV replication, viral RNA was extracted from the culture supernatants and was tested

191    by RT-PCR. The presence of PHEV particles in the infected cells was also examined by EM.

192    The EM results showed multiple virus particles approximately 110 to 130 nm in diameter with

193    typical coronavirus morphology (Fig.5D). Thus, the PHEV strain was successfully isolated and

194    was designated as PHEV-CC14.

195        Plaque assay was used to plaque isolates and to purify PHEV on Neuro-2a cells, and large

196    clear plaques were evident under an agar overlay medium on the cells. The cloned virus PHEV-

197    CC14 was tested by RT-PCR and was further serially passaged to 20 passages on Neuro-2a cells

198    ($5.2 \log_{10}$ PFU/mL). During the serial passages, significant increases in viral RNA titers were

199    observed following each cell passage. The infectious titers of PHEV-CC14 were determined by

200    $TCID_{50}$ and were calculated according to the Reed-Muench method. As shown in Figure 6, there

201    were no significant differences in replication or proliferation between the PHEV-CC14 and

202    HEV-67N strains in the Neuro-2a cells, but the RNA virus titers in the PHEV-CC14-infected

203    cells ($10^{6.03} TCID_{50}$/mL) were slightly higher than those in the HEV 67N-infected cells

204    ($10^{5.43} TCID_{50}$/mL) after 72 h post-inoculation.

205    **Sequence and phylogenetic analysis**

206        To examine whether genetic changes occurred in the PHEV-CC14 strain (GenBank:

207    KU127229) compared with other PHEVs available in GenBank, the major structure genes were

208  amplified by specific primers (Table 3) and sequenced. A total of 8,123 nucleotides were

209  determined for strain PHEV-CC14, covering five complete structure genes -- HE, S, E, M and N

210  – and the locations of the organization of the targeted genes were sketched in a conceptual map

211  (Fig.7A). Therewith, the corresponding nucleotides and deduced amino acid sequences of the

212  PHEV-CC14 strain were compared with the homologous sequences of PHEVs. The results

213  showed that the PHEV-CC14 strain shared 95%-99.2% nt identities with the other PHEV strains

214  available in GenBank. The structural genes of the PHEV-CC14 strain had the greatest nucleotide

215  sequence similarity (99.2%) to the HEV-JT06 strain (GenBank: ED919227.1), and it shared 99%

216  with HEV 67N (GenBank: AY078417.1). Compared with the HEV 67N strain, there were four

217  nucleotide sense mutations at positions 12 and 114 in the HE gene, 381 in the S gene, 146 in the

218  M gene. These nucleotide changes all induced corresponding amino acid (aa) changes (S12G and

219  T114I in the HE protein; R381H in the S protein; A146T in the M protein). However, residues in

220  the E and N genes of PHEV-CC14 strains were highly conserved in identity with other PHEV

221  reference strains in the GenBank database.

222      A phylogenetic tree was constructed using the five genes (HE, S, E, M, and N) of PHEV-

223  CC14 with some other PHEV strains obtained from GenBank Database, as well as several

224  members of the coronaviruses (Fig.7B). Phylogenetic analysis of the five genes clearly showed

225  that the PHEV-CC14 strain clustered into a subclass with a HEV-JT06 strain from China isolated

226  in 2006, and a similar finding showed that the PHEV stains in China were highly homologous

227  with a North American strain (AY078417). Additionally, the homology of the deduced amino

228    acid sequences between the PHEV-CC14 strain and HCoV-OC43 (GenBank: KF530085) was as

229    high as 91%.

## Discussion

230

231    In March 2014, there was a suspected outbreak of PHEV infection on a farm in Changchun

232    in the Jilin province of China. The clinical signs consisted of vomiting, twitching, wasting, and

233    diarrhea were observed in suckling piglets. The histologic autopsy showed that there were

234    pinpoint petechiae in the kidneys, thinning of the intestinal wall, and hemorrhage in the brain.

235    Due to the great similarity between PHEV and pseudorabies virus (PRV) infection in piglets, it

236    was difficult to distinguish them only by clinical and autopsy symptoms. Therefore, PRV and

237    PHEV were first detected by PCR and RT-PCR, respectively, and the test results showed that

238    PRV was negative, and PHEV was positive, thus excluding PRV infection. At the same time, no

239    sow abortions or stillbirth phenomena were found in the pigs, also supporting the above results.

240    Immunohistochemical staining results further confirmed PHEV infection in the brains of the

241    dead piglets. Vomiting and neurological symptoms are common in piglets infected with PHEV,

242    but the symptom of diarrhea is relatively rare. Because the outbreak was characterized by

243    vomiting and diarrhea, some other viral infections with similar clinical symptoms have been

244    reported in pigs, including PEDV, TGEV and DPCoV (Ma et al. 2015; Song et al. 2015; Tanaka

245    et al. 2015). In this study, these viruses were further detected to exclude misdiagnosis or mixed

246    infection. Thus, the case was identified as simple PHEV infection, and we successfully isolated a

247    PHEV field strain as PHEV-CC14.

248    PHEV has a typical neural tropism, and it invades the central nervous system via the

249    peripheral nervous system (Hirano et al. 2004; Lafaille et al. 2015; Lee et al. 2011; Zhang et al.

250  2014). Previous studies have shown that the virus successfully killed 1- to 8-week-old mice

251  readily by different routes, and viral antigen was detected in both peripheral nerves and the CNS

252  (Hirano et al. 2001; Hirano et al. 1995; Hirano et al. 2006). In this paper, three-week-old

253  BALB/c mice were chosen for inoculation with PHEV-CC14 by the intranasal route, and the

254  results of the experiment confirmed that PHEV-CC14 had strong pathogenicity to mice.

255  Viral titers of PHEV-CC14 or HEV 67N were determined by $TCID_{50}$, and the growth curve

256  showed that there was no significant difference in replication or proliferation between them. To

257  characterize the virus isolates, the complete structural genes were sequenced and analyzed, and

258  the phylogenetic relationships among the coronavirus strains were determined. Phylogenetic

259  trees showed that the wild type and HEV-JT06 shared the highest homology, and that identified

260  with HEV 67N was 99%. These findings suggested that PHEV strains currently circulating in

261  China are closely related. Notably, the PHEV strain JT06 isolated from Jilin province, China, in

262  2006 was most closely related to the emerging PHEV-CC14 strains, suggesting that they could

263  be derived from a similar ancestral strain. Furthermore, we performed sequence alignment and

264  homology analysis between PHEV-CC14 and other coronaviruses, which including MHV,

265  BCoV, HCoV-OC43 and Bat CoV, and we found it shared up to 91% homology with HCoV-

266  OC43 (GenBank: KF530085) (Gonzalez et al. 2003; Li 2015; Snijder et al. 1993). This finding

267  suggested that, although PHEV infection in humans has not been reported currently, there is a

268  definite potential threat to human health.

269    According to the deduced amino acids of the PHEV-CC14 strains, genetic evolution and

270    variation analyses were performed. It was found that the broad variation occurred in the encoded

271    structural proteins and functional region. There were five major structural proteins of PHEV, HE,

272    S, E, M and N proteins, encoded from 5'UTR to 3'UTR (Vijgen et al. 2006; Weiss & Navas-

273    Martin 2005). Sequence analyses of the five structural proteins of the PHEV-CC14 field isolate

274    suggested that PHEV has remained more genetically stable in the E, M and N proteins (Schultze

275    et al. 1990; Vieler et al. 1995). The HE proteins of some coronaviruses are involved in the

276    release of virions from the host cell, and it has been shown to have acetylesterase activity and to

277    function as a receptor-destroying enzyme, which might be related to the early adsorption of

278    coronavirus (Schultze et al. 1991). Compared with HEV 67N, there were two amino acids (S12G,

279    T114I) in the HE protein of PHEV-CC14 that were meaningful mutations, while six amino acid

280    variations were observed (S12G,S15G,K49N,T114I,V116A,L161F) when blasted with

281    the IAF-404 strain. We hypothesize that the amino acid variation of the HE protein might have a

282    certain effect on replication and virulence, but it was difficult to explain the differences in

283    virulence among the pigs, based on the amino acid changes. In addition, there were some

284    variations of the amino acids in the S protein, which plays vital roles in viral entry, cell-to-cell

285    spread, and the determination of tissue tropism (Dong et al. 2015; Lu et al. 2015). Therefore, the

286    differences in virulence of PHEV strains might be caused by multiple factors, and the variation

287    of the whole genome has resulted in changes in their antigenic differences.

288    **Conclusions**

289    Briefly, the outbreak on the pig farm in northern China was caused by PHEV, and the virus

290    was isolated, systematically characterized and designated PHEV-CC14. This work will enrich

291    the data on the genome and molecular epidemiology of PHEV and will provide material for

292    further study of the virulence of PHEV, which should have a certain theoretical and practical

293    significance.

294    **References**

295    Andries K, and Pensaert M. 1981. Vomiting and wasting disease, a coronavirus infection of pigs.

296        *Advances in experimental medicine and biology* 142:399-408.

297    Andries K, and Pensaert MB. 1980. Immunofluorescence studies on the pathogenesis of

298        hemagglutinating encephalomyelitis virus infection in pigs after oronasal inoculation.

299        *American journal of veterinary research* 41:1372-1378.

300    Chen K, Zhao K, Song D, He W, Gao W, Zhao C, Wang C, and Gao F. 2012. Development and

301        evaluation of an immunochromatographic strip for rapid detection of porcine

302        hemagglutinating encephalomyelitis virus. *Virology journal* 9:172. 10.1186/1743-422X-9-

303        172

304    Dong B, Gao W, Lu H, Zhao K, Ding N, Liu W, Zhao J, Lan Y, Tang B, Jin Z, He W, and Gao F.

305        2015. A small region of porcine hemagglutinating encephalomyelitis virus spike protein

306        interacts with the neural cell adhesion molecule. *Intervirology* 58:130-137.

307        10.1159/000381060

308    Dong B, Lu H, Zhao K, Liu W, Gao W, Lan Y, Zhao J, Tang B, Song D, He W, and Gao F. 2014.

309     Identification and genetic characterization of porcine hemagglutinating encephalomyelitis

310     virus from domestic piglets in China. *Archives of virology* 159:2329-2337. 10.1007/s00705-

311     014-2070-y

312  Gao W, Zhao K, Zhao C, Du C, Ren W, Song D, Lu H, Chen K, Li Z, Lan Y, Xie S, He W, and

313     Gao F. 2011. Vomiting and wasting disease associated with hemagglutinating

314     encephalomyelitis viruses infection in piglets in Jilin, China. *Virology journal* 8:130.

315     10.1186/1743-422X-8-130

316  Gonzalez JM, Gomez-Puertas P, Cavanagh D, Gorbalenya AE, and Enjuanes L. 2003. A

317     comparative sequence analysis to revise the current taxonomy of the family Coronaviridae.

318     *Archives of virology* 148:2207-2235. 10.1007/s00705-003-0162-1

319  Greig AS, Mitchell D, Corner AH, Bannister GL, Meads EB, and Julian RJ. 1962. A

320     Hemagglutinating Virus Producing Encephalomyelitis in Baby Pigs. *Canadian journal of*

321     *comparative medicine and veterinary science* 26:49-56.

322  Hirano N, Haga S, Sada Y, and Tohyama K. 2001. Susceptibility of rats of different ages to

323     inoculation with swine haemagglutinating encephalomyelitis virus (a coronavirus) by various

324     routes. *Journal of comparative pathology* 125:8-14. 10.1053/jcpa.2001.0471

325  Hirano N, Nomura R, Tawara T, Ono K, and Iwasaki Y. 1995. Neuronal spread of swine

326     hemagglutinating encephalomyelitis virus (HEV) 67N strain in 4-week-old rats. *Advances in*

327     *experimental medicine and biology* 380:117-119.

328  Hirano N, Nomura R, Tawara T, and Tohyama K. 2004. Neurotropism of swine

329     haemagglutinating encephalomyelitis virus (coronavirus) in mice depending upon host age

330    and route of infection. *Journal of comparative pathology* 130:58-65.

331    Hirano N, and Ono K. 1998. A serological survey of human coronavirus in pigs of the Tohoku

332    District of Japan. *Advances in experimental medicine and biology* 440:491-494.

333    Hirano N, Taira H, Sato S, Hashikawa T, and Tohyama K. 2006. Antibody-mediated virus

334    clearance from neurons of rats infected with hemagglutinating encephalomyelitis virus.

335    *Advances in experimental medicine and biology* 581:391-394. 10.1007/978-0-387-33012-

336    9_69

337    Lafaille FG, Ciancanelli MJ, Studer L, Smith G, Notarangelo L, Casanova JL, and Zhang SY.

338    2015. Deciphering Human Cell-Autonomous Anti-HSV-1 Immunity in the Central Nervous

339    System. *Frontiers in immunology* 6:208. 10.3389/fimmu.2015.00208

340    Lee H, Sunden Y, Ochiai K, and Umemura T. 2011. Experimental intracerebral vaccination

341    protects mouse from a neurotropic virus by attracting antibody secreting cells to the CNS.

342    *Immunology letters* 139:102-109. 10.1016/j.imlet.2011.05.008

343    Li F. 2015. Receptor recognition mechanisms of coronaviruses: a decade of structural studies.

344    *Journal of virology* 89:1954-1964. 10.1128/JVI.02615-14

345    Li YC, Bai WZ, Hirano N, Hayashida T, Taniguchi T, Sugita Y, Tohyama K, and Hashikawa T.

346    2013. Neurotropic virus tracing suggests a membranous-coating-mediated mechanism for

347    transsynaptic communication. *The Journal of comparative neurology* 521:203-212.

348    10.1002/cne.23171

349    Lu G, Wang Q, and Gao GF. 2015. Bat-to-human: spike features determining 'host jump' of

350    coronaviruses SARS-CoV, MERS-CoV, and beyond. *Trends in microbiology* 23:468-478.

351     10.1016/j.tim.2015.06.003

352   Ma Y, Zhang Y, Liang X, Lou F, Oglesbee M, Krakowka S, and Li J. 2015. Origin, evolution,

353     and virulence of porcine deltacoronaviruses in the United States. *mBio* 6:e00064.

354     10.1128/mBio.00064-15

355   Mengeling WL, Boothe AD, and Ritchie AE. 1972. Characteristics of a coronavirus (strain 67N)

356     of pigs. *American journal of veterinary research* 33:297-308.

357   Pensaert MB, and Callebaut PE. 1974. Characteristics of a coronavirus causing vomition and

358     wasting in pigs. *Archiv fur die gesamte Virusforschung* 44:35-50.

359   Quiroga MA, Cappuccio J, Pineyro P, Basso W, More G, Kienast M, Schonfeld S, Cancer JL,

360     Arauz S, Pintos ME, Nanni M, Machuca M, Hirano N, and Perfumo CJ. 2008.

361     Hemagglutinating encephalomyelitis coronavirus infection in pigs, Argentina. *Emerg Infect*

362     *Dis* 14:484-486. 10.3201/eid1403.070825

363   Rho S, Moon HJ, Park SJ, Kim HK, Keum HO, Han JY, Van Nguyen G, and Park BK. 2011.

364     Detection and genetic analysis of porcine hemagglutinating encephalomyelitis virus in South

365     Korea. *Virus genes* 42:90-96. 10.1007/s11262-010-0551-y

366   Roe CK, and Alexander TJ. 1958. A Disease of Nursing Pigs Previously Unreported in Ontario.

367     *Canadian journal of comparative medicine and veterinary science* 22:305-307.

368   Sasseville AM, Gelinas AM, Sawyer N, Boutin M, and Dea S. 2001. Biological and molecular

369     characteristics of an HEV isolate associated with recent acute outbreaks of encephalomyelitis

370     in Quebec pig farms. *Advances in experimental medicine and biology* 494:57-62.

371   Schultze B, Hess G, Rott R, Klenk HD, and Herrler G. 1990. Isolation and characterization of the

372    acetylesterase of hemagglutinating encephalomyelitis virus (HEV). *Advances in experimental*

373    *medicine and biology* 276:109-113.

374    Schultze B, Wahn K, Klenk HD, and Herrler G. 1991. Isolated HE-protein from

375    hemagglutinating encephalomyelitis virus and bovine coronavirus has receptor-destroying

376    and receptor-binding activity. *Virology* 180:221-228.

377    Snijder EJ, Horzinek MC, and Spaan WJ. 1993. The coronaviruslike superfamily. *Advances in*

378    *experimental medicine and biology* 342:235-244.

379    Song D, Moon H, and Kang B. 2015. Porcine epidemic diarrhea: a review of current

380    epidemiology and available vaccines. *Clinical and experimental vaccine research* 4:166-176.

381    10.7774/cevr.2015.4.2.166

382    Tanaka Y, Sasaki T, Matsuda R, Uematsu Y, and Yamaguchi T. 2015. Molecular

383    epidemiological study of feline coronavirus strains in Japan using RT-PCR targeting nsp14

384    gene. *BMC veterinary research* 11:57. 10.1186/s12917-015-0372-2

385    Vieler E, Schlapp T, Anders C, and Herbst W. 1995. Genomic relationship of porcine

386    hemagglutinating encephalomyelitis virus to bovine coronavirus and human coronavirus

387    OC43 as studied by the use of bovine coronavirus S gene-specific probes. *Archives of*

388    *virology* 140:1215-1223.

389    Vijgen L, Keyaerts E, Lemey P, Maes P, Van Reeth K, Nauwynck H, Pensaert M, and Van Ranst

390    M. 2006. Evolutionary history of the closely related group 2 coronaviruses: porcine

391    hemagglutinating encephalomyelitis virus, bovine coronavirus, and human coronavirus OC43.

392    *Journal of virology* 80:7270-7274. 10.1128/JVI.02675-05

393    Weiss SR, and Navas-Martin S. 2005. Coronavirus pathogenesis and the emerging pathogen

394       severe acute respiratory syndrome coronavirus. *Microbiology and molecular biology reviews :*

395       *MMBR* 69:635-664. 10.1128/MMBR.69.4.635-664.2005

396    Zhang L, Xu MM, Zeng L, Liu S, Liu X, Wang X, Li D, Huang RZ, Zhao LB, Zhan QL, Zhu D,

397       Zhang YY, Xu P, and Xie P. 2014. Evidence for Borna disease virus infection in

398       neuropsychiatric patients in three western China provinces. *European journal of clinical*

399       *microbiology & infectious diseases : official publication of the European Society of Clinical*

400       *Microbiology* 33:621-627. 10.1007/s10096-013-1996-4

402    **Legends**

403    **Fig.1** Macropathologic images of  PHEV infection in piglets from a farm in China. **(A)** The dead

404    piglets with vomiting, neurologic symptoms, wasting, and diarrhea. **(B)** Pathologic autopsy

405    showed congestion or hemorrhage in brain tissue.

406    **Fig.2** Samples submitted for histopathologic examination by hematoxylin-eosin staining and

407    IHC assay. **(A)** A large number of glial cells aggregating in the infected brains formed glial

408    nodules (arrow); hematoxylin-eosin stain, x100. A boxed inset in the lower-right panel is shown

409    at greater magnification in the image. **(B)** Brain samples in the healthy pig were normal;

410    hematoxylin-eosin stain, x400. **(C)** The PHEV infected neurons showed shrunken,

411    karyopyknosis and deeply stained (arrow); hematoxylin-eosin stain, x400. **(D)** Neurons in brain

412    of healthy pig were well-arranged and distributed evenly and orderly; hematoxylin-eosin stain,

413    x400. **(E)** Brains from an infected piglet showing PHEV-positive labeling in the cytoplasm of

414    nerve cells (arrows); immunohistochemical staining, x400. **(F)** No PHEV-positive labeling of

415    neurons in the negative control group; immunohistochemical staining, x400.

416    **Fig.3** Mice experimentally infected with PHEV-CC14. **(A)** PHEV-CC14-infected mice showed

417    arched waists, standing and vellicating front claws after at 3 dpi. **(B)** Mice in the control group

418    survived normally. **(C)** Survival curves of BALB/c mice. n=10 mice per group; three

419    independent experiments.

420    **Fig.4** Visualization of PHEV-CC14-infected brains from BALB/c mice by immunofluorescent

421    assay using PHEV monoclonal antibody (diluted 1:500). Immunofluorescent assay in the

422    cerebral cortex, showing large numbers of PHEV-positive neurons (red); original magnification,

423    ×100. PHEV-positive Purkinje cells of the cerebellum were distributed widely (red); original

424    magnification, ×400.

425    **Fig.5** Isolation and propagation of PHEV in Neuro-2a cells. **(A)** Mock-inoculated Neuro-2a cells

426    showing normal cells at 4 dpi, ×200. **(B)** CPE of PHEV-CC14-inoculated Neuro-2a cells at 4 dpi,

427    showing rounded and clustered cells, ×200. **(C)** Detection of PHEV isolate in Neuro-2a cells by

428    immunofluorescent staining using PHEV monoclonal antibody (diluted 1:500), showing

429    immunofluorescent-positive staining mainly evident in the cytoplasm of infected cells (red),

430    ×400. **(D)** EM of PHEV-CC14-inoculated Neuro-2a cells. Crown-shaped spikes are visible. The

431    samples were negatively stained with 3% phosphotungstic acid. The magnification bar in the

432    picture represents 100 nm in length.

433    **Fig. 6** The growth curves of PHEV strains. Neuro-2a cells were, respectively, inoculated with

434    PHEV-CC14 and HEV 67N. The $TCID_{50}$ was measured at different time points, and the growth

435    curves were plotted. There was no significant difference in replication or proliferation between

436    the PHEV-CC14 strain and HEV-67N strain (p>0.05).

437    **Fig.7** Protein structure prediction and phylogenetic analysis. **(A)** Schematic illustration of the

438    organization of the targeted genes coding for the five structural proteins, consisting of PHEV HE,

439    S, E, M and N genes (reference virus HEV-67N). (B) Phylogenetic analyses based on amino acid

440    sequences of the five major structural proteins from PHEV in this study (indicated with triangle)

441    and other published PHEV sequences, as well as related coronaviruses. Reference sequences

442    obtained from GenBank are indicated by strain names and accession numbers. The trees were

443    constructed using the neighbor-joining method in MEGA software, version 6.06. Bootstrap

444    analysis was performed on 1,000 trials, and values are indicated adjacent to the branching points.

445

Macropathologic images of PHEV infection in piglets from a farm in China

**Fig.1** Macropathologic images of PHEV infection in piglets from a farm in China. **(A)** The dead piglets with vomiting, neurologic symptoms, wasting, and diarrhea. **(B)** Pathologic autopsy showed congestion or hemorrhage in brain tissue.
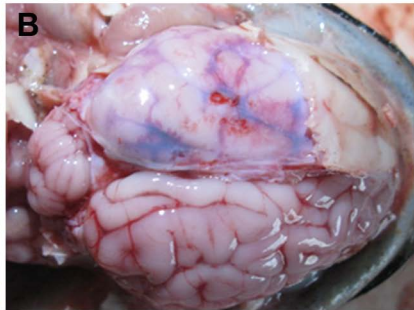
Samples submitted for histopathologic examination by hematoxylin-eosin staining and IHC assay

**Fig.2** Samples submitted for histopathologic examination by hematoxylin-eosin staining and IHC assay. (**A**) A large number of glial cells aggregating in the affected brains formed glial nodules (arrow) ; hematoxylin-eosin stain, x100.  (**B**) Brain samples in the control group were normal; hematoxylin-eosin stain, x400. (**C**) Brains from an affected piglet showing PHEV-positive labeling in the cytoplasm of nerve cells (arrows); immunohistochemical staining, x400. (**D**) No PHEV-positive labeling of neurons in the negative control group; immunohistochemical staining, x400.
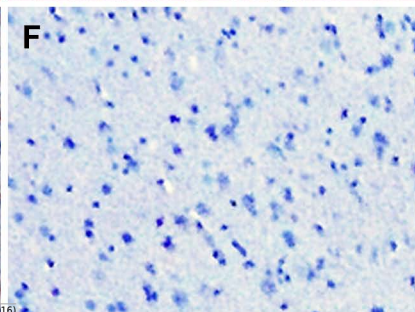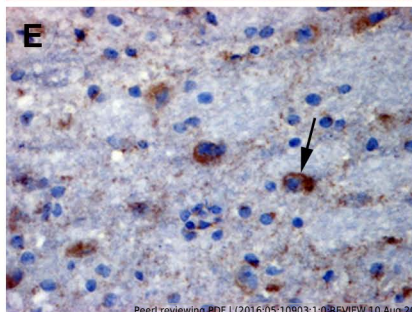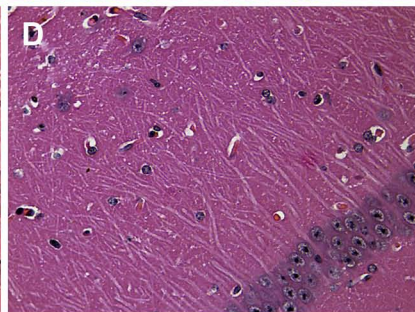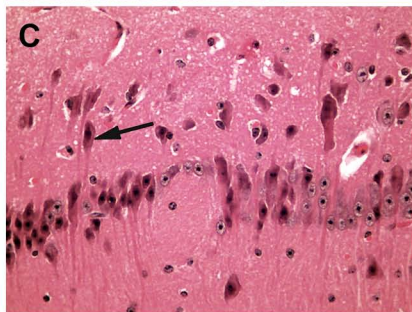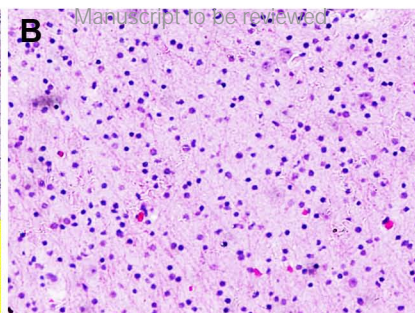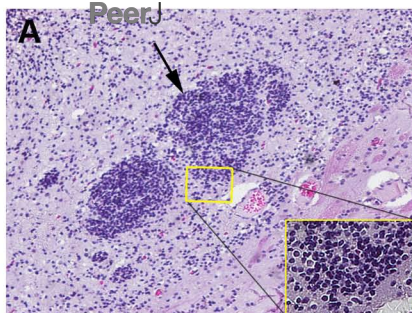
Mice experimentally infected with PHEV-CC14.

**Fig.3** Mice experimentally infected with PHEV-CC14. **(A)** PHEV-CC14-infected mice showed arched waists, standing and vellicating front claws after at 3 dpi. **(B)** Mice in the control group survived normally. **(C)** Survival curves of BALB/c mice. n=10 mice per group; three independent experiments.
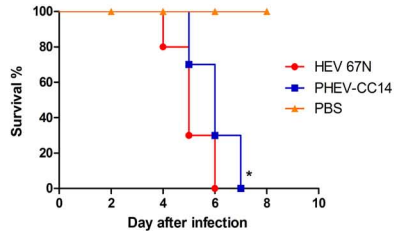
Visualization of PHEV-CC14-infected brains by IF assay

**Fig.4** Visualization of PHEV-CC14-infected brains from BALB/c mice by immunofluorescent assay using PHEV monoclonal antibody (diluted 1:500). Immunofluorescent assay in the cerebral cortex, showing large numbers of PHEV-positive neurons (red); original magnification, ×100. PHEV-positive Purkinje cells of the cerebellum were distributed widely (red); original magnification, ×400.
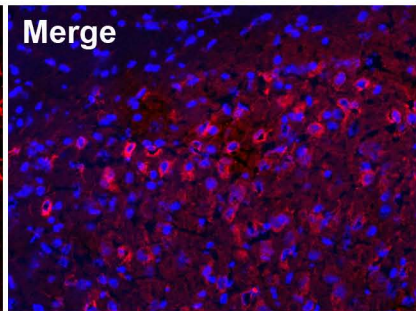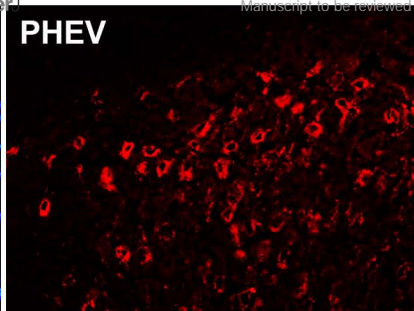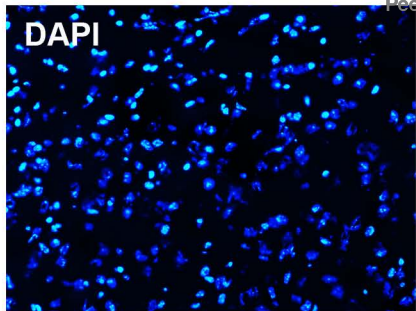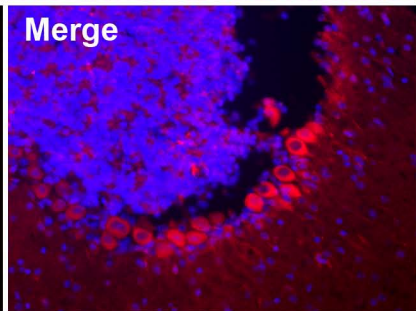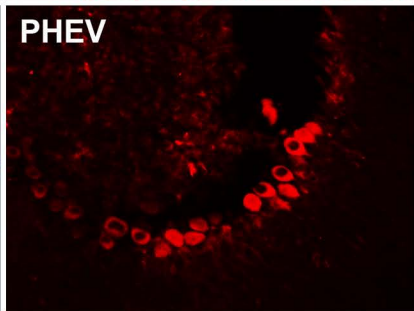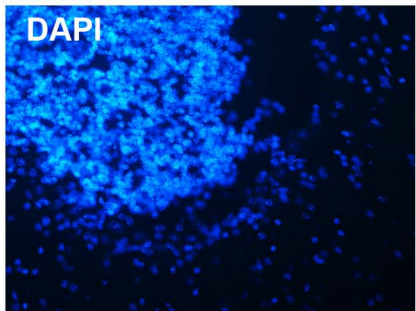
Isolation and propagation of PHEV in Neuro-2a cells.

**Fig.5** Isolation and propagation of PHEV in Neuro-2a cells. **(A)** Mock-inoculated Neuro-2a cells showing normal cells at 4 dpi, ×200. **(B)** CPE of PHEV-CC14-inoculated Neuro-2a cells at 4 dpi, showing rounded and clustered cells, ×200. **(C)** Detection of PHEV isolate in Neuro-2a cells by immunofluorescent staining using PHEV monoclonal antibody (diluted 1:500), showing immunofluorescent-positive staining mainly evident in the cytoplasm of infected cells ( red), ×400. **(D)** EM of PHEV-CC14-inoculated Neuro-2a cells. Crown-shaped spikes are visible. The samples were negatively stained with 3% phosphotungstic acid . The magnification bar in the picture represents 100 nm in length.
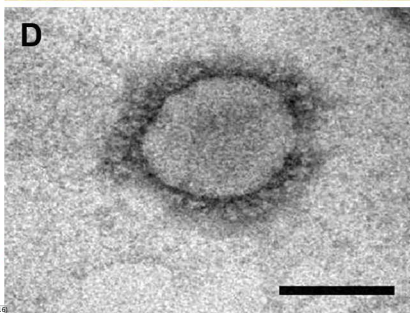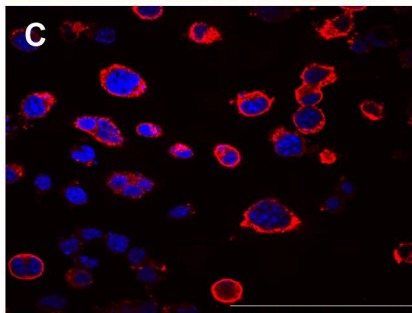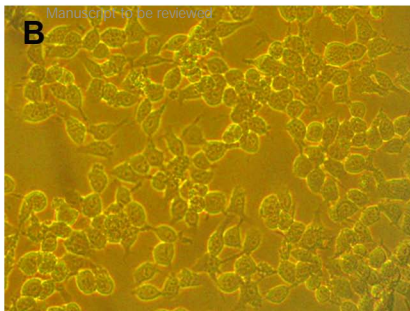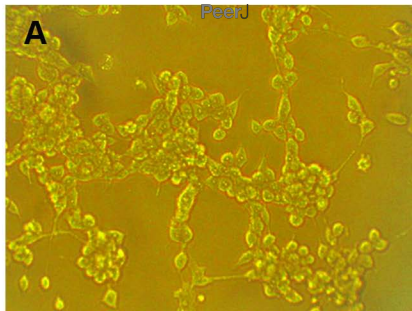
The growth curves of PHEV strains.

**Fig. 6** The growth curves of PHEV strains. Neuro-2a cells were, respectively, inoculated with PHEV-CC14 and HEV 67N. The $TCID_{50}$ was measured at different time points, and the growth curves were plotted. There was no significant difference in replication or proliferation between the PHEV-CC14 strain and HEV-67N strain ($p>0.05$).
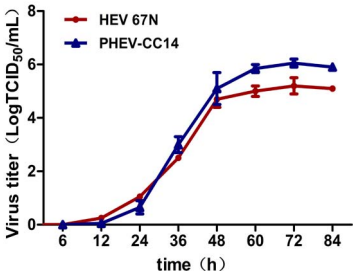
Protein structure prediction and phylogenetic analysis.

**Fig.7** Protein structure prediction and phylogenetic analysis. **(A)** Schematic illustration of the organization of the targeted genes coding for the five structural proteins, consisting of PHEV HE, S, E, M and N genes (reference virus HEV-67N). (B) Phylogenetic analyses based on amino acid sequences of the five major structural proteins from PHEV in this study (indicated with triangle) and other published PHEV sequences, as well as related coronaviruses. Reference sequences obtained from GenBank are indicated by strain names and accession numbers. The trees were constructed using the neighbor-joining method in MEGA software, version 6.06. Bootstrap analysis was performed on 1,000 trials, and values are indicated adjacent to the branching points.
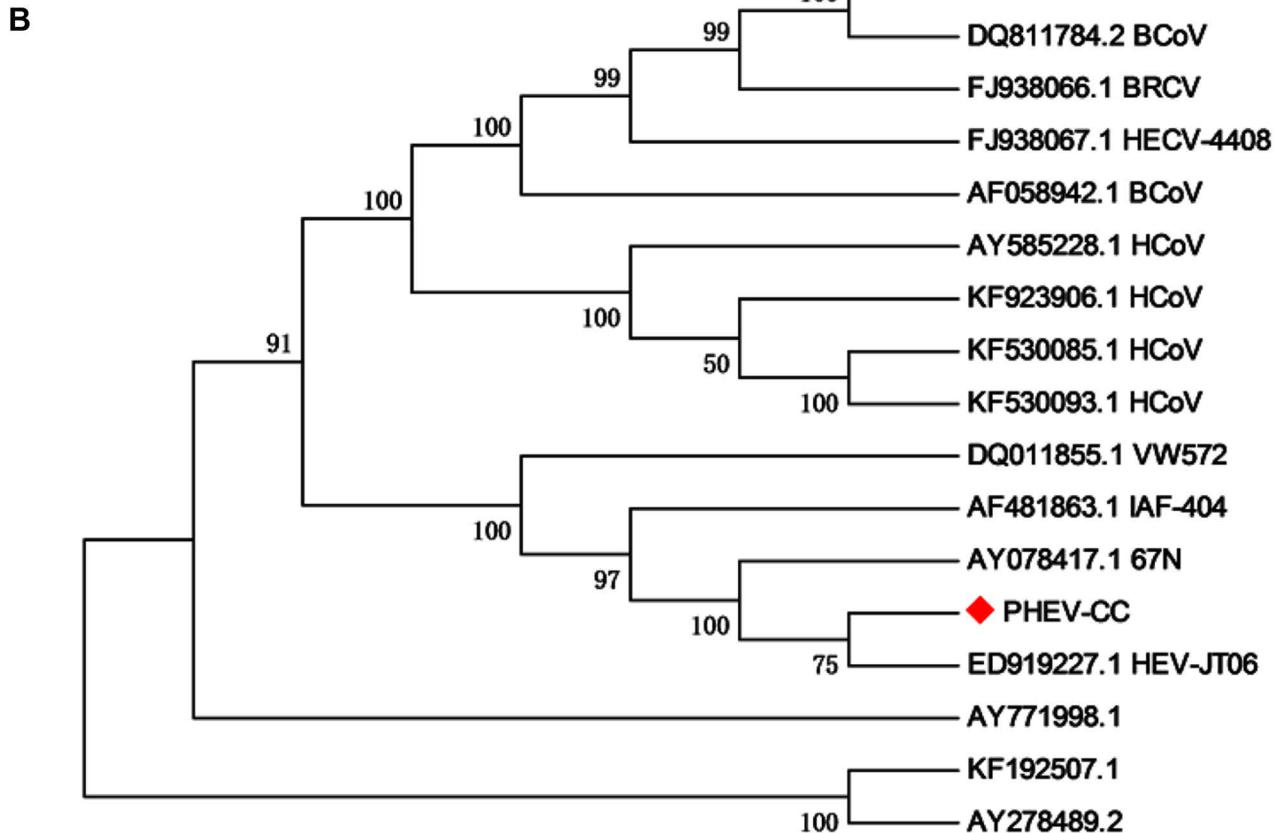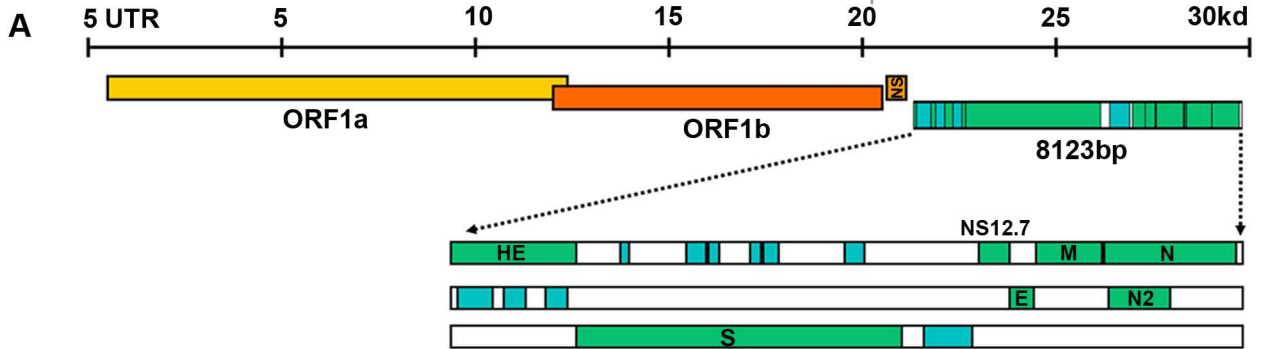
Primer sets used for RT- PCR to differential diagnosis.

1 **Table 1 Primer sets used for RT- PCR to differential diagnosis**

| Virus | Primers Sequence (5′-3′) | GenBank No, | Tm | Gene | Fragment (bp) |
|-------|--------------------------|-------------|-----|------|---------------|
| PHEV | TACTGAAACCATTACCACT CTATAACTATGACCGCGAC | AY078417.1 | 56 | HE | 509 |
| PEDV | GAAATAACCAGGGTCGTGGA GCTCACGAACAGCCACA | DQ355221.1 | 55.3 | N | 492 |
| TEGV | GATGGCGACCAGATAGAAGT GCAATAGGGTTGCTTGTACC | AF302264.1 | 58 | N | 612 |
| DPCoV | CGCGTAATCGTGTGATCTATGT CCGGCCTTTGAAGTGGTTAT | KJ569769 | 57.4 | M | 541 |
| PRV | CCGGCCTTTGAAGTGGTTAT CGACCTGGCGTTTATTAACCGAGA | M61196.1 | 56 | gH | 355 |

RT-PCR detection of PHEV and other relevant viruses on tissues.

1   **Table 2 RT-PCR detection of PHEV and other relevant porcine viruses on tissue samples**
2   **from nine pigs in Jilin province, China**

| Pig age | Original samples | PHEV and relevant porcine virus detection No. (% positive) | | | | |
|---|---|---|---|---|---|---|
| | | PHEV | PEDV | TEGV | DPCoV | PRV |
| 1-week old | brain | 6 | - | - | - | - |
| | spinal cord | 6 | - | - | - | - |
| | IC [a] | 4 | - | - | - | - |
| | spleen | - | - | - | - | - |
| | kidneys | - | - | - | - | - |
| | lungs | - | - | - | - | - |
| < 3-week old | brain | 2 | - | - | - | - |
| | spinal cord | 2 | - | - | - | - |
| | IC [a] | - | - | - | - | - |
| | spleen | - | - | - | - | - |
| | kidneys | - | - | - | - | - |
| | lungs | - | - | - | - | - |

3   [a] IC, intestinal contents.

Sequences of the oligonucleotides for gene-walking RT-PCR.

1    **Table 3 Sequences of the oligonucleotides for gene-walking RT-PCR**

| Primers | Primers Sequence (5′-3′) | Gene | Fragment (bp) |
|---|---|---|---|
| P1/P2 | TACTGAAACCATTACCACT<br>CTATAACTATGACCGCGAC | I | 1275 |
| P3/P4 | GAAATAACCAGGGTCGTGGA<br>GCTCACGAACAGCCACA | II | 1614 |
| P5/P6 | GATGGCGACCAGATAGAAGT<br>GCAATAGGGTTGCTTGTACC | III | 1674 |
| P7/P8 | CGCGTAATCGTGTGATCTATGT<br>CCGGCCTTTGAAGTGGTTAT | IV | 1390 |
| P9/P10 | CCGGCCTTTGAAGTGGTTAT<br>CGACCTGGCGTTTATTAACCGAGA | V | 256 |
| P11/P12 | ATGAGTAGTCCAACTACAC<br>TATTTCTCAACAATGCGGTGTC | VI | 685 |
| P13/P14 | TCAGGCATGGACACCGCATT<br>AGAGTGCCTTATCCCGACTTT | VII | 1463 |
| P15/P16 | TTACAGCACTTAGATCACGTAGAT<br>TAAACTCTGGCTTCGCCAGGTAAT | VIII | 2195 |